

Observation of a Natural Particle Transport Barrier in HL-2A Tokamak

W.W. Xiao 1), X.L. Zou 2), X.T. Ding 1), L.H. Yao 1), B.B. Feng 1), X.M. Song 1), S.D. Song 2), Y. Zhou 1), Z.T. Liu 1), H.J. Sun 1), Y.D. Gao 1), L.W. Yan 1), Q.W. Yang 1), Yi Liu 1), J.Q. Dong 1), X.R. Duan 1), Yong Liu 1), C.H. Pan 1) and HL-2A team

- 1) Southwestern Institute of Physics, P.O. Box 432, Chengdu, China
- 2) Association Euratom-CEA, CEA/DSM/IRFM, CEA/Cadarache, 13108 S^t Paul-lez-Durance, France

e-mail contact the main author: xiaoww@swip.ac.cn

Abstract. In this paper we report the observation of a natural generated internal particle transport barrier (pITB) in purely Ohmically heated plasmas in the HL-2A tokamak. The pITB have been observed when the line average electron density exceeds a threshold, which is $n_e=2.2\times 10^{19}m^{-3}$. The phenomenon is perfectly reproducible and identified by profile analysis, perturbative transport studies with Supersonic Molecular Beam Injection (SMBI) modulation and the Doppler reflectometry. The influence of the ECRH heating on pITB will be also presented in this paper. The barrier is generally located around $\rho= 0.65-0.7$ with a width of 1-2 cm. Especial analysing the propagation of a particle wave generated by SMBI modulation across the barrier, the particle diffusivity and the convective velocity have been separately determined. The diffusivity is rather will-like than step-like and lower in the zone of barrier than outside. The convection is inward outside of the barrier, while the convection is outward inside the barrier. The experimental results have been compared to an analytical model for particle transport to quantitatively characterize this barrier. A satisfactory agreement has been found between the experimental points and the analytical calculation. The change of sign for the convective velocity has been explained by the turbulence TEM/ITG system. The density threshold in pure Ohmic discharge may be correlated to the TEM/ITG transition via the collisionality. Some possibilities of the mechanism leading to the pITBs formation have been discussed and need further experiments to be confirmed.

1. Introduction

Intensive effort to understand the particle transport processes has been made for experimental as well as theoretical studies in tokamaks, which has direct impact on subjects as energy confinement, particle fuelling, impurity control, *etc.* This is partly because the energy economy is of the utmost importance for a viable fusion reactor. Particle transport barriers with energy confinement improvement have been observed in tokamaks, as the H-mode [1] at the edge of the plasma and ITB [2-6] in the core. These regimes have been often obtained with high power external input auxiliary heating as the neutral beam injection [1, 5], off-axis minority ion-cyclotron heating [3, 4], or large external input particle source as the pellets [2].

Mechanisms responsible for these barriers are reversed magnetic shear, or $E \times B$ rotation shear. In this paper we report the observation of a natural generated particle transport barrier in pure Ohmic discharge in HL-2A tokamak. We also present the influence of the ECRH heating on particle transport barrier. Some potent experimental evidences and analysis of the experimental results about the particle transport barrier are included.

2. Arrangements of the experiments in HL-2A

HL-2A tokamak is a middle size fusion device [7]. The main experimental parameters in the present experiments are: major radius $R=1.64\text{ m}$, minor radius $a=0.40\text{ m}$, toroidal magnetic field $B_T=1.45\text{ T}$, plasma current $I_p=185\text{ kA}$. The plasma density profile is measured by an O-mode reflectometry of 26.5-40GHz, which covers a density domain of $0.8\text{-}2.0 \times 10^{19}\text{ m}^{-3}$. The plasma turbulence poloidal rotation velocity is measured by a Doppler reflectometry system which has 8 steps by computer controlled in one shot and the frequency range of the Doppler reflectometry system is from 26GHz to 38GHz. The line averaged density is measured by a HCN interferometer. The density modulation is generated by the SMBI system [8]. ECRH heating experiments have been successfully operated in HL-2A tokamak. The microwave frequency of the ECRH system is 68GHz, the total output ECRH power is 2MW. In the present experiment, the second harmonic X-mode is applied and corresponding to the cut off density is $2.9 \times 10^{19}\text{ m}^{-3}$ and B_T is 1.21T respectively.

3. Experimental results

3.1. Density profile analysis for the pITB

Internal particle transport barriers (pITBs) have been observed in Ohmic plasmas in HL-2A with standard gas puffing when the line average electron density exceeds a defined threshold. This phenomenon is perfectly reproducible. Fig.1 shows the temporal evolution of the density profile at selected time for a typical discharge with transition to pITB, when the density ramp increases slowly: before the appearance of the transport barrier (+250 ms); at the beginning of the formation of the barrier (Δ 420 ms); strong barrier (\circ 480 ms); just after injection of a particle pulse by the SMBI (\square 520 ms). The barrier is located around $r=29\text{ cm}$. The parameter characterizing the pITB is the normalised density gradient $-a \nabla n_e/n_e=a/L_n$. Fig.2 c displays a 2-D image of the normalised density gradient, showing clearly the trace of pITB around $r=29\text{ cm}$. Before $t=400\text{ ms}$, no clear barrier has been observed. Starting from this time, the pITB appears progressively. The critical density corresponding to this transition is $\langle n_e \rangle = 2.2 \times 10^{19}\text{ m}^{-3}$. After the injection of a particle pulse using SMBI at $t=510\text{ ms}$, identified by a sharp increase of the H_a signal, the pITB trace is much more visible, and the density gradient is steeper. This is a strong indication of the presence of the transport barrier. It should be emphasized that the Mirnov coil signal shows no change during the pITB transition (Fig.2 b). Hence this pITB is not due to MHD activities.

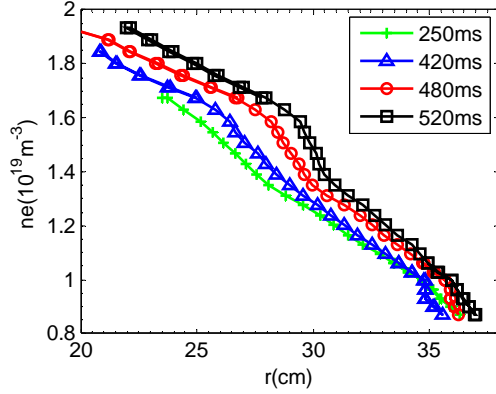


FIG. 1. Shot #7557. Temporal evolution of the density profile at selected times. Before the appearance of the barrier (+ 250 ms); at the beginning of the formation of the barrier (Δ 420 ms); strong barrier (\circ 480 ms); just after a particle pulse injected by SMBI (\square 520 ms).

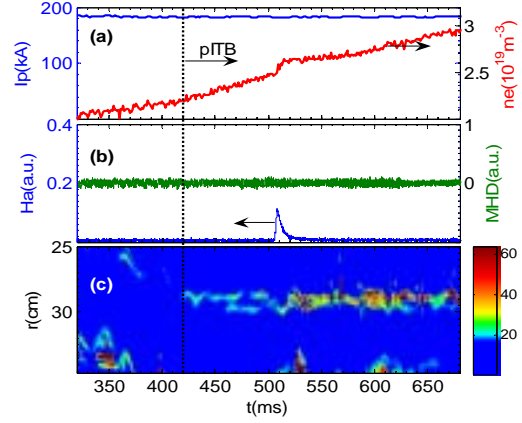


FIG. 2. Shot #7557. (a) Temporal evolution of the plasma current I_p (kA), the central line averaged density n_l ($10^{19}m^{-3}$). (b) Temporal evolution of the Mirnov coil signal and H_a signal. (c) 2-D image of the density gradient.

Fig. 3 shows the density gradient length at $t=465ms$. The width of the barrier is 1~2 cm. A drastic change has been observed in the density gradient through this barrier: $L_n \approx 10cm$ at the barrier location, $L_n \approx 50cm$ inside the barrier, and $L_n \approx 25cm$ outside the barrier. In a region without particle sources and in steady state, the particle flux $\Gamma = -D \nabla n_e/n_e - Vn_e \approx 0$, where D is the particle diffusivity, V is the particle convective velocity defined as positive for inward pinch, and negative for outward. Thus the ratio D/V is directly equal to L_n , $L_n = D/V$. The shape of the density gradient length gives interesting indications on the feature of D or V . Thus the barrier observed here is well-like and not step-like.

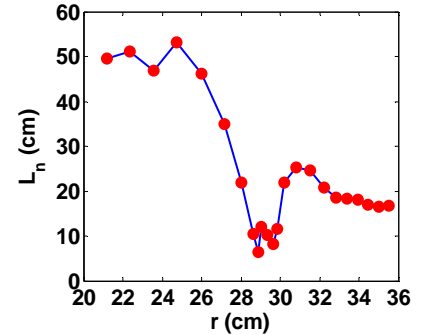


FIG. 3. Shot #7557. Density gradient length at $t=465ms$.

3.2. Density modulation analysis for the pITB

A simple profile analysis does not allow to separate D and V . Modulation of auxiliary heating (ECRH, ICRH) is a powerful tool for the investigation of the heat transport [9-11] and the heat ITB [12]. In our experiments, the density modulation has been generated by SMBI. These experiments allow normally to separate the diffusivity term and the convection term, by using the fact that on one hand the phase of the particle wave generated by the modulation is very sensitive to the diffusivity but less sensitive to the convection, and on the other hand the amplitude of the particle wave is sensitive to diffusivity but very sensitive to the convection [9].

In the present case, the SMBI modulation frequency is 9.6 Hz, the duration of SMBI pulse is

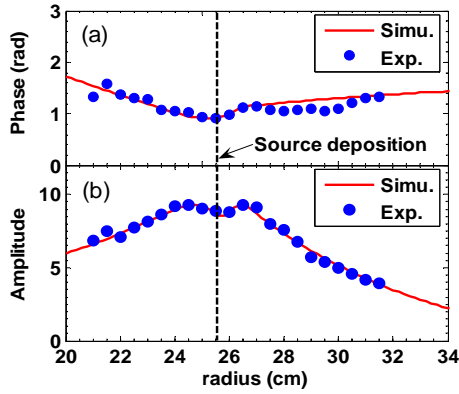


FIG. 4. Shot #7593. Phase (a), amplitude (b) of the 1st harmonic of the Fourier transform of the modulated density. Comparison between experiment (circle) and simulation (solid).

about 6 ms, the gas pressure of SMBI is 1.3 MPa. The time resolution of the reflectometry is 1 ms. Profile analysis shows a pITB around $r \approx 26-27\text{cm}$. The figures 4a, 4b display respectively the phase and the amplitude of the 1st harmonic of the Fourier transform of the modulated density. From Fig. 4a, the minimum of the phase is at $r \approx 25.3\text{cm}$, which generally determines the particle source location. The shape of the phase around the minimum gives a rough estimate of the width of the particle source. From Fig.4b, a first peak in amplitude has been found at $r \approx 24\text{cm}$, slightly shifted inwards compared to the particle source location. This indicates the presence of a significant particle pinch in this region. At the barrier location $r \approx 27\text{cm}$, a second peak has been found in the amplitude, and strong effect has been observed in the phase.

Now the experimental results have been compared to an analytical model [13] for particle transport to quantitatively characterize this barrier. In cylindrical geometry the particle transport equation is simply given by: $\frac{\partial n_e}{\partial t} = \frac{1}{r} \frac{\partial}{\partial r} \left[rD \frac{\partial n_e}{\partial r} + rVn_e \right] + S(r, t)$ with the following

control parameters, the diffusivity D and the convective velocity V . S is the particle source. For the simulation, the following parameters are used: the modulation frequency $f_0=9.6\text{Hz}$, the particle deposition $r_{dep}=25.3\text{cm}$, the minor radius $a=40\text{cm}$, the transport barrier is between $x_1=25.6\text{cm}$ and $x_2=26.7\text{cm}$, the particle source is given by a Gaussian distribution with the amplitude $S_0=0.69 \times 10^{19} \text{m}^{-1}\text{s}^{-1}$ (the total particle injected per second is $N_p=2\pi RS_0$), and the width $w = 0.03a$. On the Fig. 4a and b, the solid lines represent the simulation. A satisfactory agreement has been found between the experimental points and the analytical calculation, and we have found Fig.5: in the domain 1 ($r < x_1$): $D_1=0.1\text{m}^2/\text{s}$, $V_1=1.0\text{m/s}$; in the domain 2 or in the well ($x_1 < r < x_2$), $D_2=0.045\text{m}^2/\text{s}$, $V_2=-2.7\text{m/s}$; in the domain 3 ($r > x_2$), $D_3=0.5\text{m}^2/\text{s}$, $V_3=6.0\text{m/s}$. In the present case the neoclassical Ware pinch [14] $V_{ware} \approx (r/a)^{0.5} E_\phi / B_\theta \approx 0.6\text{m/s}$ around the barrier, where E_ϕ is the toroidal electric field, and B_θ is the poloidal magnetic field. The pinch velocity found in the domain 3 is much larger than the Ware pinch, while the velocity found in the domain 1 is very close to the latter. For comparison, SMBI modulations have been also performed for a discharge with a density $\langle n_e \rangle = 1.9 \times 10^{19} \text{m}^{-3}$ lower than the critical value. In this case, no barrier has been observed and the diffusivity obtained by this method is $D=0.25\text{m}^2/\text{s}$, for $r=28-31\text{cm}$, and a negative convective velocity has been found $V = -2.2\text{m/s}$ for $r=28-31\text{cm}$, $V=-4.2\text{m/s}$ for $r=31-33\text{cm}$.

The convective velocity obtained above, using SMBI modulation, can be connected to the turbulent transport models. In tokamaks, an anomalous particle pinch exists in addition to the

neoclassical Ware pinch as shown in [15, 16]. Theoretical works have shown that this anomalous particle pinch can be driven by turbulence and is composed by two terms: the curvature driven pinch $V_q = C_q D \nabla q/q$, and the thermodiffusion one $V_T = -C_T D \nabla T_e/T_e$. In the plasma core ($r/a < 0.80$), the electron particle transport is mainly governed by two turbulences: the ion temperature gradient driven modes (ITG), and the electron trapped mode (TEM). As shown in [17, 18], for electrons V_q always points inwards, whereas the thermodiffusion term can change direction according to the kind of turbulence: positive or inward for ITG, and negative or outward for TEM. As shown in ASDEX_U for Ohmic discharges [19], TEM is dominating for low collisionality (density), while ITG is dominating for high collisionality (density). The TEM/ITG transition occurs for an effective collisionality $\nu_{eff}^* \approx 10$ ($\rho = 0.6-0.7$). The effective collisionality is defined as $\nu_{eff}^* = \nu_{ei}/\omega_{De} \approx 10^{-14} R Z_{eff} n_e T_e^{-2}$, where ν_{ei} is the e-i collision frequency, ω_{De} is the drift frequency, R is the major radius in m , Z_{eff} is the effective ion charge, n_e is the density in m^{-3} , T_e is the electron temperature in eV . Applying to our case at $\rho = 0.7$, $R = 1.64m$, $Z_{eff} \approx 1.5$, $n_e = 1.5 \times 10^{19} m^{-3}$, $T_e = 0.2 keV$, the effective collisionality corresponding to the density threshold is $\nu_{eff}^* \approx 9$, very close to that for TEM/ITG transition. Thus the explanation for the convective velocity found with SMBI modulation could be the following: under the density threshold, TEM is the dominant turbulence, and the convective velocity is negative since the thermodiffusion is dominating. Beyond the threshold, the dominant turbulence is the ITG mode, the convective velocity with thermodiffusion dominance is positive. Inside the transport well, as shown in [20], TEM can be driven by the steep density gradient when a/L_n exceeds a critical value $(a/L_n)_{crit} \approx 1.6$. In the present case $a/L_n \approx 4$ much larger than the critical value, thus the corresponding convective velocity is negative inside the transport well.

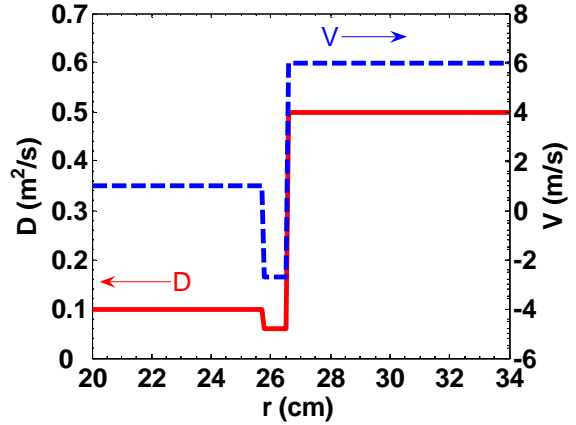


FIG. 5. Diffusivity D (solid), convective velocity V (dash) for the simulation of shot #7593.

3.3. The turbulence perpendicular rotation analysis for the pITB

In order to know if the formation of the pITB is linked or not to the $E \times B$ rotation shear, the turbulence perpendicular rotation velocity has been measured with the Doppler reflectometry [21]. The probed turbulence wavenumber is about $k_s = 5-9 cm^{-1}$, which is in the wavenumber range for ITG and TEM. Fig. 6 shows the radial profile of the perpendicular rotation velocity of the turbulence for different densities. Below the critical density $\langle n_c \rangle = 2.2 \times 10^{19} m^{-3}$, the measured velocity is smoothly increasing with radius for $0.6 < r/a < 0.9$. When the line average density exceeds the density threshold, a drastic change in the measured rotation velocity has been observed in the barrier region $r/a = 0.6-0.7$. We have also plotted in Fig.6 the electron diamagnetic drift velocity V_e^* , which is computed from the measured density and electron

temperature profiles. Same feature is observed in the barrier region for V_e^* . Assuming $V = V_{E \times B} + V_e^*$, from Fig.6 we have roughly $V_{E \times B} \approx 1 \text{ km/s}$ for $0.6 < \rho < 0.9$. This suggests that the

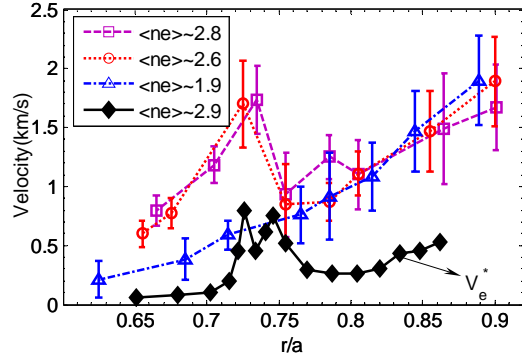


FIG. 6. Radial profile of the perpendicular turbulence rotation velocity with pITB (\circ, \square) without pITB (Δ) measured by Doppler reflectometry. Radial profile of the electron diamagnetic drift velocity V_e^* .

drastic change observed in the turbulence rotation velocity at the barrier results is from the steepness of the density gradient in the barrier.

3.4. The influence of ECRH heating on the pITB

The comparative experiments have been done concerning both Ohmic phase and ECRH phase. The main aim is to know the influence of the ECRH heating on the particle transport barrier. The experimental results in ECRH heating show that the density profiles are different from the

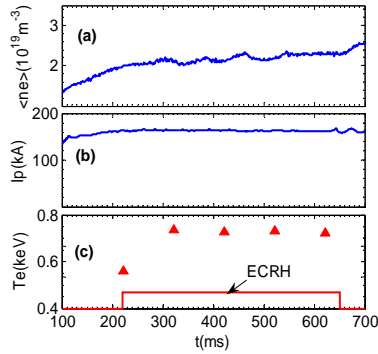


FIG. 7. The evolution of the parameters in ECRH heating in shot 8264: (a) the line average density by HCN, (b) the plasma current and (c) the electron temperature by Thomson scattering.

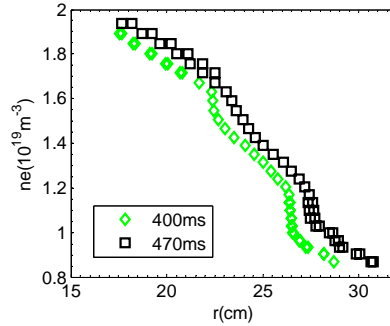


FIG. 8. The density profile by microwave reflectometry in different time in shot 8264. The particle transport barrier position is about $r=26 \text{ cm}$. Line average density is about $2.2 \times 10^{19} \text{ m}^{-3}$, the power of the ECRH heating is about 200 kW.

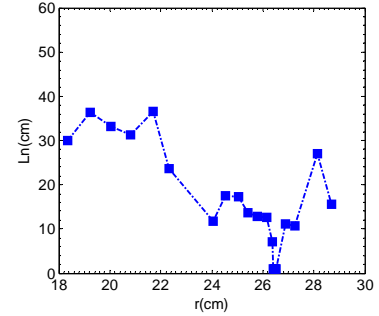


FIG. 9. The density gradient length of shot 8264 at $t=400 \text{ ms}$. The minimum value is smaller than value in figure 3. It shows that the particle transport barrier in ECRH is stranger than that in pure Ohmic discharge.

Ohmic phase: under same line average density conditions, the local density at the pITB foot in ECRH heating is lower ($1.0 \times 10^{19} \text{ m}^{-3}$) than that in Ohmic discharge ($1.4 \times 10^{19} \text{ m}^{-3}$). Fig. 7 shows the time evolution of the average density measured by HCN interferometer (a), the plasma current (b) and the temperature measured by Thomson scattering (c) in shot 8264. On-axis ECRH heating switch on from 220 ms in this shot. Before ECRH the plasma line

average density just reaches the critical density $2.2 \times 10^{19} m^{-3}$ as shown in figure 7(a). The density profiles in the region of the particle transport barrier during ECRH heating are steeper than that in shot 7557 as shown in Fig. 8 and Fig. 1, respectively. The density gradient length has also been calculated as shown in figure 9. The values of the density gradient length in the particle transport barrier are lower than the values of in shot 7557 in the barrier zone. But the positions of the pITB are almost in the same place, around $\rho=0.65\sim 0.7$.

4. Summary

The pITB phenomena have been experimentally observed in the core region of Ohmic plasmas in HL-2A tokamak. A density threshold has been found for the formation of the pITB with $\langle n_e \rangle = 2.2 \times 10^{19} m^{-3}$. The diffusivity D is rather well-like than step-like. The convection is inward outside of the well and outward inside the well. The change of sign for the convective velocity has been explained by the turbulence TEM/ITG system. During the formation of the barrier, neither magnetic shear nor $E \times B$ rotation shear underwent great change. On the other hand the formation of this barrier coincides with the TEM/ITG transition. The pITB may be created initially by the discontinuity or jump in the convective velocity during the TEM/ITG transition. These could have interesting implication for the control of the particle transport barrier via turbulence. The influence of the ECRH heating on the particle transport barrier has been also observed: **i)** the density profiles in the region of the particle transport barrier are steeper in ECRH heating than that in Ohmic phase; **ii)** under same line average density conditions, the local density at the pITB foot in ECRH heating is lower than that in purely Ohmic discharge.

The authors would like to thank Dr. X. Garbet and Dr. G. Giruzzi for fruitful discussions and to thank HL-2A team.

References

- [1] F. Wagner, G. Faussmann, D. Grave *et al.*, Phys. Rev. Lett. **53**, (1984) 1453
- [2] M.J. Greenwald, D.A. Gwinn, S. Milora *et al.*, Phys. Rev. Lett. **53**, (1984) 352
- [3] C.L. Fiore, J.E. Rice, P.T. Bonoli *et al.*, Phys. Plasmas **8**, (2001) 2023
- [4] J.E. Rice, P.T. Bonoli, E.S. Marmor *et al.*, Nucl. Fusion **42**, (2002) 510
- [5] E.J. Doyle, G.M. Staebler, L. Zeng *et al.*, Plasma Phys. Controlled Fusion **42**, (2000) A237
- [6] D.R. Baker *et al.*, Nuclear Fusion, Vol. 40, No. 5, IAEA, Vienna, (2000) 1003
- [7] Y. Liu *et al.*, Nucl. Fusion **45** (2005) 239
- [8] L.H. Yao *et al.*, Nucl. Fusion **38**, (1998) 631
- [9] N.J. Lopes Cardozo, Plasma Phys. Control. Fusion **37**, (1995) 799
- [10] P. Mantica, G. Gorini, G.M.D. Hogeweij *et al.*, Phys. Rev. Lett. **85**, (2000) 4534

- [11] F. Ryter, F. Leuterer, G. Pereverzev *et al.* Phys. Rev. Lett. **86**, (2001) 2325
- [12] P. Mantica, D. Van Eester, X. Garbet *et al.*, Phys. Rev. Lett. **96**, 095002 (2006)
- [13] S.P. Eury, E. Harauchamps, X.L. Zou *et al.*, Phys. Plasmas **12**, 102511 (2005)
- [14] A.A. Ware, Phys. Rev. Lett. **25**, (1970) 916
- [15] G.T. Hoang, C. Bourdelle, X. Garbet *et al.*, Phys. Rev. Lett. **90**, 155002 (2003)
- [16] A. Zabolotski, H. Weisen, TCV Team, Plasma Phys. Control. Fusion **45**, (2003) 735
- [17] X. Garbet, L. Garzoti, P. Mantica *et al.*, Phys. Rev. Lett. **91**, 035001 (2003)
- [18] C. Bourdelle, X. Garbet, F. Imbaux *et al.*, Phys. Plasmas **14**, 112501 (2007)
- [19] G.D. Conway, C. Angioni, R. Dux *et al.*, Nucl. Fusion **46**, (2006) 799
- [20] D.R. Ernst, P.T. Boloni, P.J. Catto *et al.*, Phys. Plasmas **11**, (2004) 2637
- [21] X.L. Zou, T.F. Seak, M. Paume *et al.*, Proc. 26th EPS Conf. on Controlled Fusion and Plasma Physics (Maastricht) Vol. 23J, (1999) 1041